
# Age hardening of the aluminium alloy EN 4017

by D.B. Swanepoel* and W.E. Stumpf*


## Synopsis

**Hulamin Rolled Products (Ltd) developed a high Mn and Si containing alloy, EN 4017 as a scrap consuming alloy from the waste generated in producing their range of clad products for brazing of inter alia automotive heat exchangers. The multifaceted composition of this alloy (Al -1.2 wt% Si -1.1 wt% Mn -0.2 wt% Mg -0.26 wt% Cu) suggested that it might display some degree of strengthening via precipitate formation of the $Mg_2Si$-types. The aging isotherms constructed showed that EN 4017 with 0.19% Mg reached a lower peak strength (YS~210 MPa and UTS~260 MPa) compared to the EN 4017 material with 0.43% Mg (YS~270 MPa and UTS~325 MPa). The higher Mg variant of EN 4017 was comparable with the age-hardenable reference alloy EN 6061. Selected area electron diffraction (SAED) studies proved that the microstructure of age hardened EN 4017 contained a combination of β', β" and U2 phase after being aged at 175ºC for 65 h. The general microstructure contained precipitate free zones as well as grain boundary Si films, although these did not lead to significant embrittlement. The role of Mn dispersoids in the fracture mechanism of 4017 is also discussed. The article will compare the behaviour of EN 4017 with that EN 6061.**


**Keywords: Age-hardening, dispersoids, magnesium silicide, precipitate free zones**

## Introduction

Hulamin Rolled Products (Ltd) currently manufactures an aluminium brazing sheet by the hot rolled cladding of a 3 series (high Mn) core with a 4 series (high Si) alloy. The recycling of scrap generated by this product resulted in an alloy containing significantly high quantities of both Si and Mn. In order to utilize this material, Hulamin developed an alloy with composition equivalent to EN 4017 (hereafter referred to as 9017) as a scrap-consuming alloy which is currently sold as building sheet. The multifaceted composition of this alloy (Al -1.2wt% Si -1.1wt% Mn -0.2wt% Mg -0.26wt% Cu) suggested that it might display some degree of strengthening via precipitate formation of the $Mg_2Si$-types. The requirement for this is, simply, that since Si is in excess if compared to a popular reference alloy 6061, sufficient Mg must be available for the formation of the strengthening precipitate $Mg_2Si$.

Precipitation processes in the Al-Mg-Si system have been extensively researched in the recent past and emphasis has been placed on the Mg:Si ratio and the effects that it has on the process and properties[1–3]. The general precipitation process is commonly accepted to follow the following sequence[2–5]:

Supersaturated Al solid solution→atomic clusters→GP-zones→β"→β'/B'→β ($Mg_2Si$)

The precipitation starts with the formation of Mg and/or Si atomic clusters depending on the Mg:Si ratio[3]. It is suggested that, essentially only Si-clusters will form in an alloy with a high concentration of excess Si. In alloys such as 9017, which have a very high relative Si content, it is stated that the excess Si will cause a higher number density of Si clusters to form (i.e. more clusters) as a result of the higher degree of Si supersaturation upon quenching[2]. The finer precipitate microstructure is then inherited by the following GP-zones and β″ which then causes a more potent degree of dislocation arrest and ultimate strengthening compared to an alloy with a similar amount of $Mg_2Si$ but a lower excess Si[5]. It is primarily β″ that is responsible for peak strength. As with most of the metastable precipitates in aluminium alloys, β″consists of needles or rods that are aligned along the <100> directions of the face centered cubic Al. They have typical diameters of 4 nm and lengths of 50 nm[6].

The majority of the 6XXX-series alloys do not contain excess Si and in the rare cases where it does, it rarely exceeds 0.6%Si. This is due to the concern that the high excess concentration will cause precipitation of primary Si on the grain boundaries and thereby lower the material's toughness arising from intergranular fracture[7].

* *Department of Materials Science and Metallurgical Engineering, University of Pretoria, South A.*

 *SA ISSN 0038–223X/3.00 + 0.00. Paper received Feb. 2009; revised paper received Jul. 2009.*

Cases of age hardening in non age hardenable families of Al alloys have been mentioned in the literature such as alloy AA 3004, containing Mg and Mn as major alloying elements, that showed an age hardening response due to the presence of as little as 0.2% Si[8]. Zhu and Starink[9] also investigated the age-hardenability of different alloys with compositions, Al –(1-3) wt% Mg –(0-0.4) wt% Cu -0.15 wt% Si -0.25 wt% Mn. They found that in the presence of Cu contents of about 0.25%, similar to 9017, hardening was induced by the formation of both $Mg_2Si$ and S-phase ($Al_2CuMg$). References by consultants to Hulamin have also been made as to the ability of alloy AA 3105 (Al -0.86%wt Mn -0.28 wt% Si -0.2 wt% Mg) to form $Mg_2Si$. Despite these observations of increases in strength due to solutionizing and aging, none of the above mentioned workers have, to the authors' knowledge, actually confirmed $Mg_2Si$ via a TEM study as the precipitate responsible for strengthening.

Despite high Mn concentrations in all the cases, the major difference between the above mentioned cases and that of 9017 lies in the fact that in the former it was Si that was the limiting reagent, whereas in 9017, it is Mg that is the limiting reagent. Although not immediately apparent, this will have a definite influence on both the expected properties as well as the precipitation processes, including raising the minimum required solutionising temperature. Similarly, based on 9017's high excess Si, it is also suggested that it will overage slower[2] compared to the experimental alloys used by the authors above[8,9].

In addition to acting as a solid solution strengthener and improving properties such as the work hardening rate[6], Mn has the tendency to also form dispersoids. These are generally formed upon reheating the ingot for hot rolling where the Mn retained in solution by the fast solidification rates of DC casting, precipitate out in the form of dispersoids with typical sizes of 0.05–0.5 μm[10]. Two types of dispersoids are found, β-$(Fe,Mn)Al_6$ and α-$Al_{12}(Fe,Mn)_3Si$. The latter type is expected in the presence of Si in the alloy whereas the former β-type, generally forms first in low Si alloys, but gradually transforms to the α-type by Si extraction from the surrounding matrix[11].

The formation of dispersoids in Al-Mg-Si alloys is generally stated to have beneficial effects in terms of toughness and fatigue resistance due to homogenization of slip in the matrix[5,12,13]. Based on literature[6], it can also be suggested that the Mn will tie up the excess Si in the matrix and, thereby, reduce the degree of grain boundary precipitation of primary Si. Some authors also mention that the dispersoids can act as nucleation sites for strengthening precipitates and, thereby, produce more homogenous precipitation in the alloy[14]. The extent of this effect is, however, uncertain since the dispersoids are generally coarse and distributed far apart compared to the strengthening precipitates. Through an Orowan based calculation, Lee *et al.*[10] attributed an additional increase in strength of 30–40 MPa to the presence of dispersoids in Al-Mg-Si alloys. The dispersoids in their case did, however, have a very high Mn:Si ratio, thereby suggesting that they are of the β-type, which is also accepted to generally be finer. It is expected that the coarser α-type dispersoids in the high Si alloy, 9017, will contribute considerably less to strengthening.

Primary Si crystals are commonly formed in alloys as rich in Si as 9017. Although these crystals have a limited effect on strengthening, they are reported to increase the work hardening rate in Al-Mg-Si alloys since their incoherent nature makes them more difficult to be sheared by passing dislocations compared to the coherent or semi-coherent precipitates[15]. It is also possible to form a quaternary Q-phase (Al-Mg-Cu-Si) in 9017. It is deduced from the work of[16] that this Q-phase can also be responsible for some degree of strengthening.

## Experimental

Two alloys, with different Mg contents and falling within the 9017 composition (Table I - referred to as 9017-HiMg and 9017-LoMg), were DC cast and hot rolled by Hulamin to a gauge of 3 mm. Alloy 6061 was used as a reference alloy.

The first part of the study involved the construction of isotherms for the aging process. Duplicate samples in both the transverse and longitudinal rolling directions were solutionized at 540°C for 15 minutes and given a water quench. The samples were then aged at 175°C for varying times after which they were quenched in water maintained at 24°C, subsequently machined into a wishbone shape (ASTM E8) and subjected to tensile testing.

Thin foils were also prepared for TEM analysis. Samples from all three the alloys were solutionised at 540°C for 30 minutes, water quenched and subsequently aged at 175°C for 1 h, 16 h and 65 h. Thinning was done in an electrolyte consisting of 5% Perchloric acid in methanol at room temperature with a Struers Electropolisher. A flow rate setting of 4 was used together with an applied voltage of 20 V which resulted in a current of about 0.2 A. The foils were then examined with a Phillips CM 20T electron microscope at an

*Table I*

**Chemical composition of the 9017 alloys as well as the EN standard and the reference 6061 alloy**

| | % | Al | Si | Fe | Cu | Mn | Mg | Cr | Zn | Ti |
|---|---|---|---|---|---|---|---|---|---|---|
| 9017-HiMg | Nom | Bal | 1.3 | 0.32 | 0.24 | 1.1 | 0.43 | 0.007 | 0.011 | 0.048 |
| 9017-LoMg | Nom | Bal | 1.2 | 0.32 | 0.26 | 1.0 | 0.19 | - | 0.017 | 0.041 |
| EN 4017 Standard | Min | Bal | 0.6 | - | 0.10 | 0.6 | 0.10 | - | | - |
| | Max | Bal | 1.6 | 0.70 | 0.50 | 1.2 | 0.50 | - | 0.20 | - |
| 6061 | Nom | Bal | 0.71 | 0.41 | 0.30 | 0.057 | 1.0 | 0.19 | 0.003 | 0.017 |

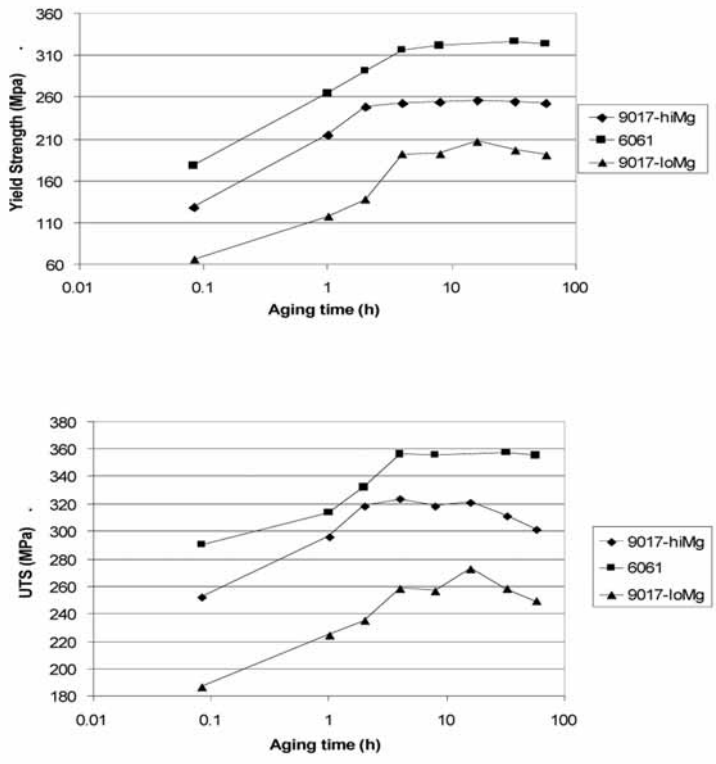


**Figure 1—Aging isotherms depicting the change in mechanical properties for 9017-HiMg, 9017-LoMg as well as that of reference alloy, 6061 aged at 175ºC**

acceleration voltage of 160 KV. The extremely small size of the precipitates, particularly the GP zones, rendered them too small to be analysed via EDX. It was, furthermore, suggested that the nanometer sized particles were even too small for analysis via replica extraction.

Selected Area Electron Diffraction (SAED) patterns were also taken from areas containing the needle-like precipitates in 9017 material aged at 175ºC for 65 h. A database with the crystallographic parameters of all the possible precipitates were generated with JEMS© software. This software calculates the expected diffraction patterns along various zone axes and conditions and superposes these on the experimental micrograph for comparison with the background pattern of the precipitates. In order to obtain a valid comparison, the camera length and other microscopic parameters were calibrated based on the FCC lattice spacings of Al for each micrograph.

## Results

The isotherms for the three alloys aged at 175ºC are shown in Figure 1. It is apparent from the isotherms that a 0.2% increase in the Mg content for alloy 9017 had a substantial effect on this alloy's ability to age harden. The average standard deviation of all the data points was 2.5 MPa, with the largest being 7.8 MPa for 6061 after 2 h of aging.

The microstructures of 9017-HiMg material in the under-, peak- and over-aged conditions are shown in Figures 2–4. The coarsening of the precipitates with aging can clearly be observed as well as the high degree of strain contrast of the precipitates in the peak aged conditions which is lost together with coherency upon further over aging. The precipitates were less clear in 9017-LoMg in the peak and under aged conditions, most likely due to the lower Mg content. The precipitates in the over aged condition did, however, have a similar appearance to 9017-HiMg except for being present in substantially smaller amounts. Visually, no Q phase precipitates were identified in the microstructures which is mentioned by Esmaeili *et al.*[16] to have a substantially longer needle length coupled with a smaller diameter.

The micrograph in Figure 4 also shows a dispersoid that was confirmed by EDX analysis to contain Al, Mn and Si. It was found that distinct precipitate free zones (PFZ) surrounded these dispersoids in the peak and over aged conditions, but were absent in the under aged condition (Figure 5). Although fewer dispersoids were present in the

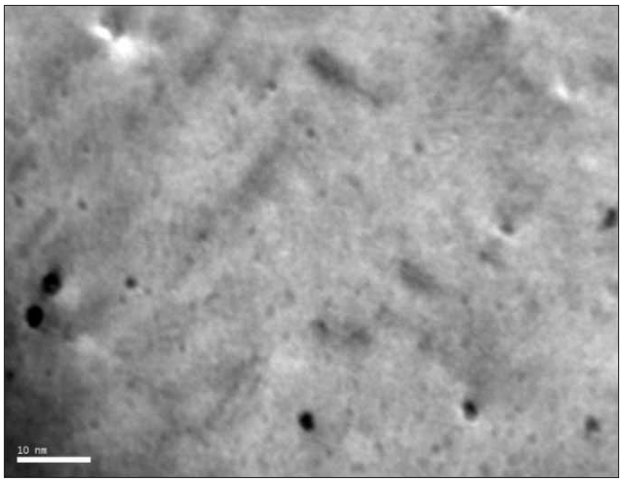


**Figure 2—TEM micrograph depicting the precipitates (GP-zones) in under-aged (1h @ 175ºC) 9017-HiMg material seen along <100>Al**

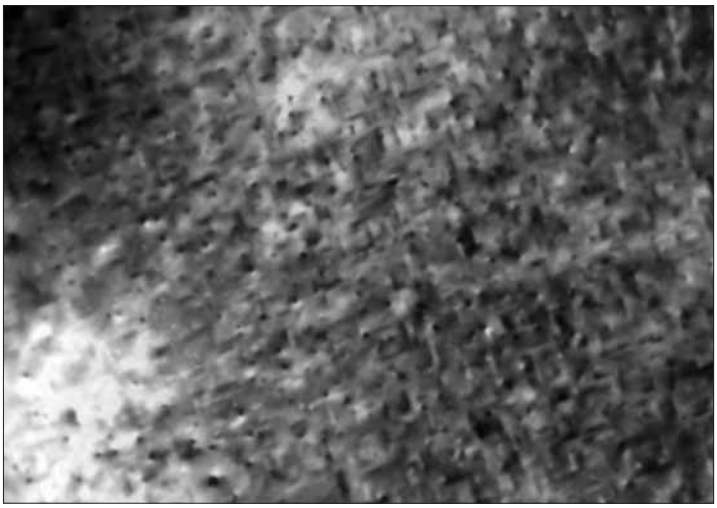

**Figure 3—TEM micrograph depicting the β" precipitates in peak-aged (8h @ 175ºC) 9017-HiMg material seen along <100>Al**

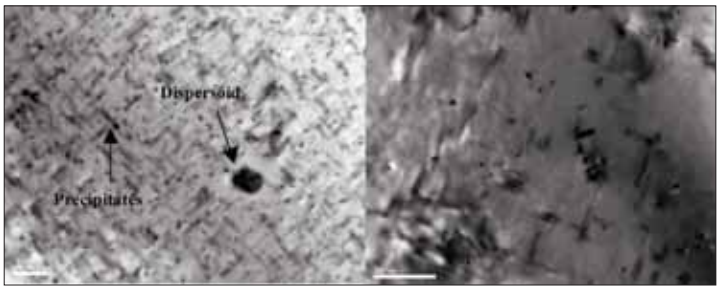


**Figure 4—TEM micrographs depicting the β'/β" precipitates in (Left) over aged (60h @ 175ºC) 9017-HiMg and (Right) over aged (60h @ 175ºC) 9017-LoMg seen along <100>$_{Al}$**

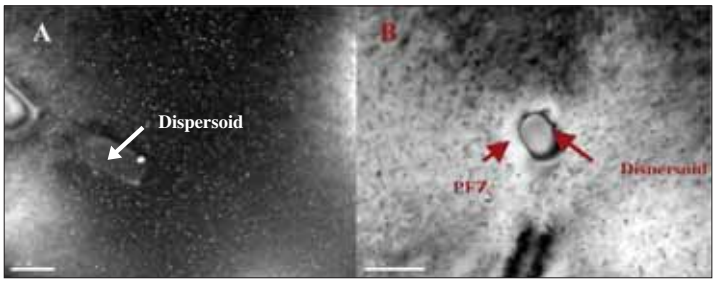


**Figure 5—TEM dark-field micrograph showing (A) the absence of a PFZ adjacent to a dispersoid in the under aged (1h @ 175ºC) compared to (B) a bright field micrograph of peak aged (8h @175ºC) 9017-HiMg**

case of 6061, they were also observed to be surrounded by PFZ's in the peak and over aged conditions but with the major difference that these dispersoids contained a considerably higher Cr content. Some dispersoids in the alloy 9017 were also identified that contained a 'cap' with a higher Si:Mn than the rest of the dispersoid (Figure 6), while primary Si crystals were also identified in the matrix. Semi continuous films of primary Si coating the grain boundaries were also observed in the case of 9017-HiMg (Figure 7), although the occurrence of these films was very scarce.

A number of experimental diffraction patterns for 9017-HiMg material in the over-aged condition (65h @ 175ºC) are superposed with the calculated diffraction patterns for various precipitates in Figure 8. It sould be mentioned that the spots were delibirately, slightly offset to enable comparison of the experimental and calculated spots.

It is clear from the results that the microstructure consisted of a mixture of hexagonal β′, monoclinic β″ and the orthorhombic U2-phase, as identified by Matsuda *et al.*[14]. The first two phases were aligned with their [101] directions along the needle lengths whereas the U2-phase had its [110] direction along its needle length. It is however not possible to rule out the presence of some Q-phase being present as this phase has an exactly equivalent crystall structure to β′.

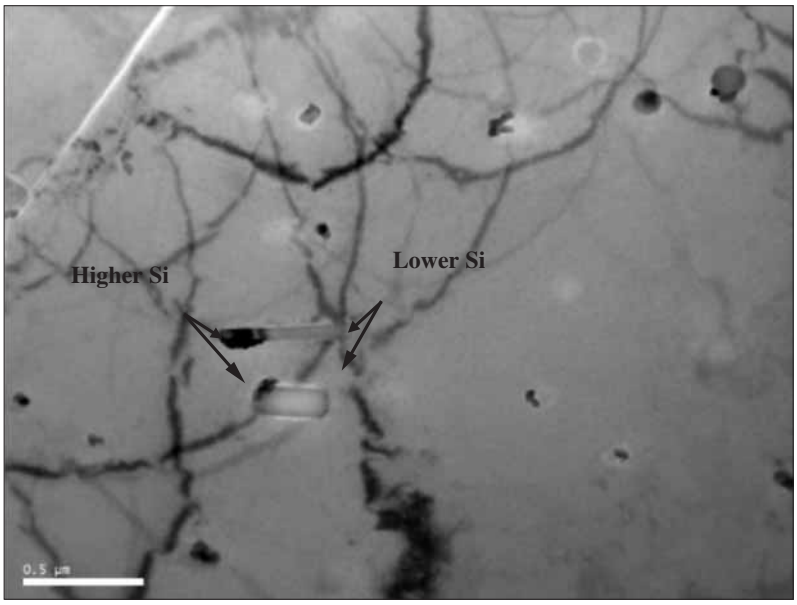


**Figure 6—TEM micrograph of in 9017-HiMg showing two dispersoids with varying Si:Mn ratios. Dark sections are of higher Si content**

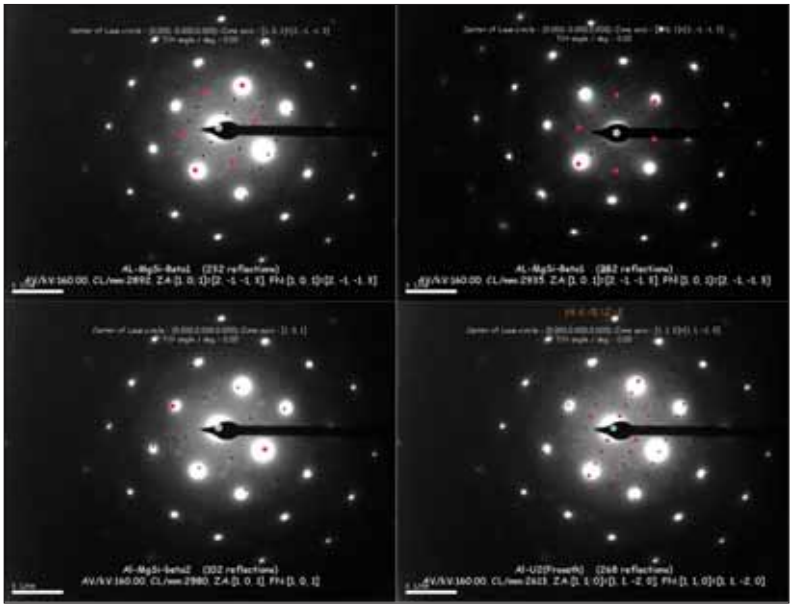

**Figure 8—Experimental SAED patterns superposed with the expected diffraction patterns. (Top: left and right) β' along the [101] zone axis. (Bottom left) β" along[101] showing the common positions of some of the spots already covered by β'. (Bottom right) U2-phase as seen along its[110] axis**

Figure 9 compares the notch sensitivity ratios ($NSR=UTS_{notched}/UTS_{unnotched}$ according to ASTM E 338) of the three different alloys under various aged conditions. The NSR of the softer 9017-LoMg was higher than for the high Mg alloy with a P-value (confidence level) of 97.8% whilst the NSR of alloy 6061 was the lowest with a P-value in excess of 99.5%. The most important fact to note is that all the NSR's of 9017 were larger than 0.88 reaching values of up to 0.995, thereby, suggesting that 9017 is not exceedingly prone to embrittlement during aging.

The fracture surfaces of all the specimens were also analysed via SEM/EDX. As Figure 10 depicts, it is evident that the final fracture mechanism consisted of a ductile fracture that consists of voids. Each void contained a secondary phase particle and EDX analysis confirmed this particle to contain Al, Mn and Si, thus suggesting that it is a dispersoid.

## Discussion

The increase in strength due to precipitate formation in the two 9017 alloys can clearly be seen from the aging isotherms. It was suggested that, if $Mg_2Si$ did form, that Mg would be the limiting reagent. The substantially higher strength of the 9017 HiMg proves that with more Mg present, a higher volume fraction of precipitates did form, thereby leading to an increased number of dislocation barriers. The

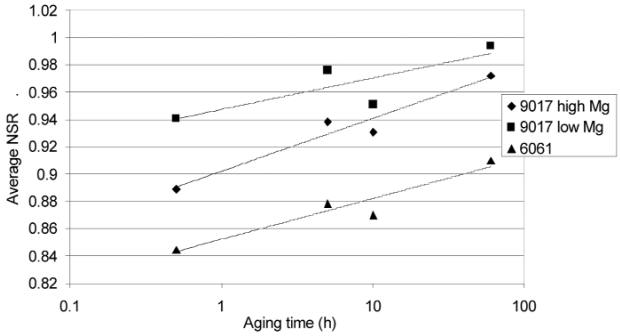


**Figure 9—Comparison of the changes in the notch sensitivity ratios (NSR) of the three alloys under various aged conditions**

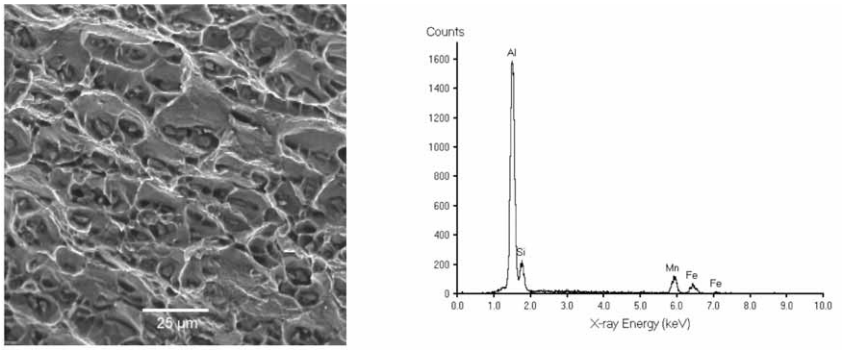


**Figure 10—(Left) SEM fractograph of 9017 Lo-Mg aged for 10 h at 175ºC. (Right) EDX spectrum of the intermetallic particles contained in each void**

alloy, 6061, however, contains Mg and Si contents that would form a higher $Mg_2Si$ fraction, thereby explaining its higher strength. As mentioned in the literature, it is also suggested that 9017 owes its unexpectedly good aging kinetics to the formation of a finer microstructure due to the excess Si.

Although the phases identified were only in the slightly over aged condition, it at least serves as proof that the strengthening precipitates are of the magnesium silicide type prevalent in 6XXX series aluminium alloys. The precipitates were, therefore, most likely preceded by the generic precipitation sequence mentioned earlier. Since the material analysed was already in the slightly over aged condition, the presence of β′ can be expected as well as some of the unaltered β″ from the peak aged condition. It has, furthermore, also been mentioned[2] that the phase, U2, is more prone to form in a Si excess environment which was the case in alloy 9017. Marioara *et al.*[2] did however, also mention that it is likely for a combination of β′, β″ and U2-phase to be present in a single needle, thereby suggesting the *in situ* nature of the transformation. As mentioned, the presence of the Q-phase can, unfortunately, not be ruled out. Since this phase does, however, only form upon transformation of β"[17], it is not expected to play a major role in the peak strength condition.

The isothermal aging behaviour can also be explained from the isothermal aging curves. In the under aged condition, the microstructure contained coherent GP zones which did not have the same strengthening potential as the slightly coarser, semi -coherent β″. Although no EDX analysis or SAED could be done on these extremely small precipitates in the under aged condition, they do at least appear exactly the same as the GP-zones in the excess Si 6XXX-series alloys of Murayama and Hono[3] and are proven to be succeeded by the more stable β′ precipitates. The decrease in strength upon further aging can be attributed to the coarsening of the precipitates which is associated with increasing the needle length, as well as losing coherency along the needle length during the transformation to β′. This reaction has also been observed in the TEM investigation.

The formation of the PFZ's adjacent to the dispersoids can be explained by the process by which the dispersoids formed upon preheating to hot rolling[14]. As was mentioned, the first dispersoids to form are generally enriched in Mn and transform to the α type by Si extraction from the matrix. The Si-'capped' particles observed in the TEM study serve as a proof of this removal of Si from the matrix. The thermally stable dispersoids are not altered significantly during the subsequent solution annealing and aging processes. The Si depleted zone still exists although there is still sufficient Si remaining for the initial Si clusters to form. Upon further aging, the clusters smaller than a critical size will revert by dissolving and aiding the larger clusters in transforming to GP-zones[18]. It was suggested by Marioara *et al.*[2] that GP zones are more stable in a matrix containing excess Si. Therefore, it is suggested that the critical radius for the clusters in the Si depleted region was larger than most precipitates in this region and that they reverted, thereby, aiding the clusters in the matrix to transform. This explains why PFZ's are present in the peak and over aged conditions but absent in the under aged condition. It was, however, interesting to note that this phenomenon is not unique to alloy 9017, but also present in 6061. The Cr rich dispersoids formed in alloy 6061 are of exactly the same α-type as in 9017 as it is possible for the Mn to be substituted by Cr in this precipitate.

The fact that the notch sensitivity ratios (NSR) are below unity suggest that a relatively small degree of brittleness is present in the material. Most of the values for 9017 did, however, approach unity with only one value below 0.93 and, therefore, it can be concluded that 9017 is not strongly embrittled by the excess Si. This fact is supported by investigation of the fracture surfaces and the absence of any primary Si on the fracture surface or any indications of intergranular fracture. Instead, the fracture occurred by the final coalescence of voids nucleated at the Al-Mn-Si dispersoids being aggravated by the presence of PFZ's in the peak- and over-aged conditions. In this mechanism, concentrated slip takes place on certain slip planes where the coherent strengthening precipitates are sheared. These dislocations then heap up at the incoherent Al-Mn-Si dispersoids where the void is ultimately nucleated[15]. Thereby, it can be concluded that the high Mn content had two beneficial effects with regards to ductility:

- It tied up the excess Si in the form of dispersoids thereby lowering the driving force for precipitation of primary grain boundary Si
- It prevented intergranular fracture by preventing the dislocations on concentrated slip planes to nucleate voids at the grain boundaries.

The higher NSR of 9017-LoMg to 9017-HiMg and 9017-HiMg to 6061 can be attributed, not necessarily to different microstructures or fracture mechanisms, but rather to the higher strength of the alloys 9017-HiMg and 6061 respectively. It is commonly known that the NSR of a material scales with its strength and that a stronger material will have a lower NSR, due to the increased resistance to material flow in the notched area[19]. Nevertheless, 6061 is not considered a brittle alloy due to the absence of any primary Si and presence of some Cr-dispersoids and since it has a lower NSR compared to 9017 one can at least suggest that 9017 is not necessarily more brittle than 6061.

## Conclusions

It can be concluded that the alloy 9017 does display age hardening behaviour up to the extent where it can even compete with commercial heat treatable 6XXX series aluminium alloys. The strengthening precipitates are confirmed to be of the same type ($Mg_2Si$) as was suggested by previous workers in the age hardening abilities of 3 series aluminium alloys containing Mg and Si. It is suggested that the high Si content was responsible for this good response in aging kinetics. Although the actual precipitation sequences are exactly the same as those mentioned for Al-Mg-Si alloys, the high Mn concentration did have secondary effects on the precipitation, such as the formation of a higher amount of dispersoids enriched in Mn compared to Cr-rich dispersoids of 6061 which were beneficial with regards to ductility. Although the fairly coarse Mn dispersoids did not contribute much to strengthening, it did play a very important role in the ductility of the alloy. The presence of PFZ's adjacent to the dispersoids is, however, not unique to 9017, as similar cases were also observed in 6061 and it is expected to have played a role in the fracture mechanism in these alloys. The excess Si did lead to the formation of some Si films on the grain boundaries, although the extent could have been more significant if the Mn did not tie up some Si in the thermally stable dispersoids, thereby, having a beneficial effect.

## Acknowledgements

The author wishes to thank Hulamin (Ltd) South Africa for their financial contributions and material supplied for this study. Special thanks are also given to Alison Tuling of IMMRI for her help with the TEM study. The permission of both Hulamin and the University of Pretoria to publish these results is also kindly acknowledged.

## References

1. Gupta, A.K., Lloyd, D.J., and Court, S.A. Precipitation hardening in Al-Mg-Si alloys with and without excess Si. *Materials Science and Engineering*, 2001, vol. A316. pp. 11–17.
2. Marioara, C.D., Andersen, S.J., Zandbergen, H.W., and Holmestad, R. The influence of alloy composition on precipitates of the Al-Mg-Si system. *Metallurgical and Materials Transactions*, 2005, vol. 36A. pp. 691–702.
3. Murayama, M. and Hono, K. Pre-precipitate clusters and precipitation processes in Al-Mg-Si alloys. *Acta Materiala*, 1999, vol. 47, no. 5. pp. 1537–1548.
4. Dutta, I. and Allen, S.M. A calorimetric study of precipitation in commercial aluminium alloy 6061. *Journal of Materials Science Letters*, 1991, vol. 10. pp. 323.
5. Dorward, R.C. and Bouvier, C. A rationalization of factors affecting strength, ductility and toughness of AA6016-type Al-Mg-Si-(Cu) alloys. *Materials Science and Engineering*, 1998, vol. A258. pp. 33–44.
6. Zandbergen, H.W., Andersen, S.J., and Jansen, J. Structure determination of Mg5Si6 Particles by dynamic electron diffraction studies. *Science*, 1997, vol. 277. pp. 1221–1225.
7. Mundolfo, L.F. Aluminium Alloys-Structure and Properties, Butterworths, London. 1976. p. 566–572.
8. Ding, S. and Morris, J.G. Processing of AA3004 alloy can stock for optimum strength and formability. *Metallurgical and Materials Transactions*, 1997, vol. 28A. pp. 2715–2721.
9. Zhu, Z. and Starink, M.J. Solution strengthening and age hardening capability of Al-Mg-Mn alloys with small additions of Cu. *Materials Science and Engineering*, 2008, vol. A 488. pp. 125–133.
10. Lee, D.H., Park, J.H., and Nam, S.W. Enhancement of Mechanical properties of Al-Mg-Si alloys by means of Manganese dispersoids. *Materials Science and Technology*, 1999, vol. 15. pp. 450–455.
11. Kuijpers, N.C.W., Vermoelen, F.J., Vuik, C., Koenis, P.T.G., Nilsen, K.E., and van der Zwaag, S. The dependence of the β-AlFeSi to α-Al(FeMn)Si transformation kinetics in Al-Mg-Si alloys on the alloying elements. *Materials Science and Engineering*, 2005, vol. A394, no. 1-2. pp. 9–19.
12. Dowling, J.M. and Martin, J.W. Influence of Mn addition on the deformation and fracture behaviour of an Al-Mg-Si alloy. *Inst Met*, 1973, vol. 1, no. 3. pp. 170–174.
13. Dowling, J.M. and Martin, J.W. Influence of Manganese additions on the deformation behaviour of an Al-Mg-Si alloy. *Acta Metall*, 1976, vol. 24, no. 12. pp. 1147–1153.
14. Matsuda, K., Ryo, F., Kawabata, T., Hiroyuki, T., Uetani, Y., and Ikeno, S. Effect of additional elements on age-hardenability of Al-Mg-Si alloys. *Journal of Light Metal Welding and Construction*, 2002, vol. 40, no. 1. pp. 19–30.
15. Zhen, L. and Kang, S.B. Deformation and Fracture behaviour of two Al-Mg-Si alloys. *Metallurgical and Materials Transactions*, 1997, vol. 28A. pp. 1489–1497.
16. Esmaeili, S., Wang, X., Lloyd, D.J., and Poole, W.J. On the precipitation-hardening behaviour of the Al-Mg-Si-Cu alloy AA6111. *Metallurgical and Materials Transactions*, 2003, vol. 34A. pp. 751–763.
17. Yassar, R.S., Field, D.P., and Weiland, H. The role of predeformation on the β" and β' precipitates and the Q' phase in an Al-Mg-Si alloy, AA6022. *Scripta Materialia*, 2005, vol. 53. pp. 299–303.
18. Miao, W.F., Laughlin, D.E., Precipitation hardening in aluminium alloy 6022. *Scripta Materialia*, 1999, vol. 40, no. 7. pp. 873–878.
19. Dieter, G.E. Mechanical Metallurgy, SI metric edition, McGraw-Hill, 1988, pp. 290-294. ◆